



HAL
open science

Proteomic analysis of *Acanthamoeba castellanii* response to *Legionella pneumophila* infection

Alban Hay, Steven Rolland, Clement Bernard, Yann Héchard, Romain Villéger, Ascel Samba-Louaka

► To cite this version:

Alban Hay, Steven Rolland, Clement Bernard, Yann Héchard, Romain Villéger, et al.. Proteomic analysis of *Acanthamoeba castellanii* response to *Legionella pneumophila* infection. *FEMS Microbiology Letters*, 2023, 10.1093/femsle/fnad086 . hal-04218559

HAL Id: hal-04218559

<https://hal.science/hal-04218559>

Submitted on 26 Sep 2023

HAL is a multi-disciplinary open access archive for the deposit and dissemination of scientific research documents, whether they are published or not. The documents may come from teaching and research institutions in France or abroad, or from public or private research centers.

L'archive ouverte pluridisciplinaire **HAL**, est destinée au dépôt et à la diffusion de documents scientifiques de niveau recherche, publiés ou non, émanant des établissements d'enseignement et de recherche français ou étrangers, des laboratoires publics ou privés.

Proteomic analysis of *Acanthamoeba castellanii* response to *Legionella pneumophila* infection.

Alban HAY¹, Steven ROLLAND¹, Clement BERNARD¹, Yann HECHARD¹, Romain VILLEGIER¹, Ascel SAMBA-LOUAKA¹

¹ Université de Poitiers, UMR CNRS 7267, Ecologie et Biologie des Interactions, France

Corresponding author: Ascel SAMBA-LOUAKA

ascel.samba@univ-poitiers.fr

Université de Poitiers

Ecologie et Biologie des Interactions UMR CNRS 7267

Microorganismes, Hôtes & Environnements team, B31 building

3 rue Jacques Fort, TSA51106

86073 POITIERS Cedex 9

Keywords: *Acanthamoeba castellanii*, *Free-living amoebae*, *Host-pathogen interaction*, *Legionella pneumophila*, *Proteomics*, *T4SS dependent*

ORIGINAL UNEDITED MANUSCRIPT

Abstract

Legionella pneumophila is an opportunistic pathogen responsible for Legionnaires' disease or Legionellosis. This bacterium is found in the environment interacting with free-living amoebae such as *Acanthamoeba castellanii*. Until now, proteomic analyses have been done in amoebae infected with *L. pneumophila* but focused on the *Legionella*-containing vacuole. In this study, we propose a global proteomic analysis of the *A. castellanii* proteome following infection with *L. pneumophila* wild-type (WT) or with an isogenic $\Delta dotA$ mutant strain, which is unable to replicate intracellularly. We found that infection with *L. pneumophila* WT leads to reduced levels of *A. castellanii* proteins associated with lipid homeostasis/metabolism, GTPase regulation and kinase. The levels of organelle-associated proteins were also decreased during infection. *L. pneumophila* WT infection leads to increase levels of proteins associated with proteins polyubiquitination, folding or degradation and antioxidant activities. This study reinforces our knowledge of this too-little-explored but so fundamental interaction between *L. pneumophila* and *A. castellanii*, to understand how the bacterium could resist amoeba digestion.

Introduction

Legionella pneumophila is a Gram-negative bacterium, found in natural and artificial aqueous environments. It can be responsible for severe pneumonia called Legionnaire's disease in humans. Transmission occurs through inhalation of contaminated aerosols and the illness is caused by the capacity of the bacterium to evade phagocytosis by alveolar macrophages. This ability is probably due to prior adaptation to intracellular growth within phagotrophic protists in their environment, such as free-living amoebae (FLA). FLA live independently in soil or water and do not require an animal host. They share the capacity to produce pseudopods, allowing them to move, via a so-called amoeboid movement, and to feed by phagocytosis on other microorganisms, mainly bacteria. More than a training ground, FLA constitute a natural host and an environmental reservoir that enhances *L. pneumophila* survival and protection against biocidal treatments, especially in anthropogenic systems like stagnant pipes or cooling towers (Berjeaud *et al.* 2016). Among FLA, *Acanthamoeba castellanii* is known to be a multiplication site for *L. pneumophila* and constitutes a good cellular model for *Legionella* infection (Swart *et al.* 2018; Samba-Louaka 2021). *A. castellanii* is found in many environments and presents a biphasic life cycle. A form called trophozoite allows its nutrition and its multiplication by binary fission. Exposure to stressful conditions results in differentiation into a resistant form called a cyst (Samba-Louaka *et al.* 2019).

L. pneumophila has evolved to disrupt certain transduction signal pathways of the host ensuring its replication. *L. pneumophila* uses a Dot/Icm type IV secretion system (T4SS), which plays a crucial role in infection. The T4SS allows *L. pneumophila* to translocate more than 300 effectors that hijack the host physiology to its advantage to grow intracellularly. They also allow the bacterium to set up a niche called a "*Legionella*-containing vacuole" (LCV) that protects against intracellular digestion. Plenty of effectors have eukaryotic protein domains that mimic those of the host (Cazalet *et al.* 2004; Gomez-Valero *et al.* 2019).

L. pneumophila infection induces host morphological changes (rounding), mobility reduction and cell cycle modification (Simon *et al.* 2015; Mengue *et al.* 2016, 2017; de Jesús-Díaz *et al.* 2017). *L. pneumophila* can disrupt several amoeba essential functions or process such as transcription, translation, cytoskeleton machinery, lipid metabolism, organelle function, autophagy, and host cell death (Yang, Li and Zhan 2022). Finally, *L. pneumophila* could egress the host by causing its lysis. If the physiology of the bacterium during the infection process has been well described, extensive studies are required to decipher the amoebae' physiological response.

Some OMIC approaches have been used to study how the bacterium hijacks *A. castellanii* metabolism. Metabolomics approaches have shown that *L. pneumophila* was able to uptake *A. castellanii* amino acids into the LCV and to use serine preferentially during the post-exponential phase of intracellular growth (Schunder *et al.* 2014; Kunze *et al.* 2021). At the transcriptomics level, in response to *L. pneumophila* infection, *A. castellanii* transcriptome was modified with LegAS4 that promotes rDNA transcription by targeting specific rDNA chromatin regions and upregulating genes linked to hydrolase activity, catalytic activity, and DNA binding while downregulating genes associated with oxidoreductase activity (Li *et al.* 2020; Moon *et al.* 2021). A study already analyzed proteome modifications following infection using 2D-DIGE and mass spectrometry analysis (Maita *et al.* 2018). However, to our knowledge, no previous study investigated the *A. castellanii* proteome modification following *L. pneumophila* infection by using a gel-free analysis.

Here, we propose for the first time, a global proteomic analysis of *A. castellanii* upon infection with *L. pneumophila*. We observed that in response to *L. pneumophila* WT infection, the levels of many host proteins were changed compared to the isogenic $\Delta dotA$ mutant. Particular attention was given to the comparison of gene ontology (GO) terms enriched when *A. castellanii* is infected with *L. pneumophila* WT versus *L. pneumophila* $\Delta dotA$. Cellular processes related to lipids and proteins and many molecular functions such as kinase activities, peptidase activities or host antioxidant activities were altered. These results open

many avenues to explore, for a better understanding, the interaction between *L. pneumophila* and a natural host *A. castellanii*.

Materials and methods

Strains, growth conditions, media, and buffer.

A. castellanii ATCC 30010 was cultured in Peptone Yeast Glucose (PYG) medium (2% proteose peptone, 0.1% yeast extract, 0.1 M glucose, 4 mM MgSO₄, 0.4 mM CaCl₂, 0.1% sodium citrate dehydrate, 0.05 mM Fe(NH₄)₂(SO₄)₂ 6H₂O, 2.5 mM NaH₂PO₃, 2.5 mM K₂HPO₃, pH 6.5) at 30°C.

L. pneumophila Paris strains were cultured on buffered charcoal yeast extract (BCYE) (1% ACES, 1% yeast extract, 0.2% charcoal, 1.5% agar, 0.025% Iron (III) pyrophosphate, 0.04% L-cysteine, 0.1% alpha-ketoglutarate, pH 6.9) agar plate. Bacteria were cultured on BCYE at 37°C for 3 days. Then, bacteria were inoculated at the optical density at 600 nm (OD₆₀₀) of 0.1 in Buffered Yeast Extract (BYE) at 37°C under agitation at 180 rpm for 21 h to reach OD₆₀₀ above 4.

L. pneumophila Paris is *L. pneumophila* Paris CIP 107629T, in the following Lp WT (Cazalet *et al.* 2004). The isogenic $\Delta dotA$ mutant of *L. pneumophila* Paris, in the following Lp $\Delta dotA$ (resistant to the kanamycin at 15 µg/mL) was a gift of Carmen Buchrieser from Pasteur Institute (Paris, France) (Gomez-Valero *et al.* 2014).

Infection of *A. castellanii* with *L. pneumophila*.

Three culture flasks (75 cm²) were inoculated for each condition: non-infected, infected with Lp WT (24 and 48 h) or Lp $\Delta dotA$ (24 and 48 h) with 4×10⁵ amoebae/flask in 30 mL of PYG medium. These flasks were incubated for 24 h at 30°C without shaking. The cell supernatant was discarded and replaced with 30 mL of a bacterial suspension of *L. pneumophila* (Lp WT or Lp $\Delta dotA$) in PYG buffer at a multiplicity of infection (MOI) of 10. These flasks were then incubated for 24 or 48 h at 30°C. Amoebae were peeled off and the amoebic suspensions

from the three flasks were pooled into one. The amoeba concentration for each suspension was quantified using a FastRead 102® counting chamber (Biosigma) and microscope.

***L. pneumophila* multiplication in *A. castellanii* cultures.**

A colony-forming unit (CFU) count was performed extemporaneously. For this purpose, 1 mL of amoebic suspension of each condition was directly lysed with a FastPrep-24™ 5G (MP Biomedicals, USA) at 5.0 m.s⁻¹ for 35 sec (3 cycles with 5 min on ice between each cycle). For the monitoring of bacteria associated with amoebae, another 1 mL of amoebic suspension was centrifuged (500×g / 5 min / RT) and washed 3 times with Page's Amoeba Saline solution (PAS) (4 mM MgSO₄, 0.4 M CaCl₂, 0.1% sodium citrate dehydrate, 2.5 mM NaH₂PO₃, 2.5 mM K₂HPO₃, pH 6.5) before lysing with FastPrep-24™ 5G as described previously. The suspensions were serially diluted and cultured on agar plates for viable counting of bacteria after three days of incubation at 37°C. A follow-up of the number of amoebae per milliliter was also carried out at 24 and 48 h p.i. by FastRead 102® counting chamber using a light microscope.

Cell viability

4×10⁵ amoebae were inoculated within 12-well plates. Cell viability of infected and non-infected cells was assessed by staining amoebae with Trypan Blue. Cell suspension samples were diluted in ratio 1:1 with Trypan Blue (0.4% Solution) and the counting was performed with a FastRead 102® counting chamber using a light microscope.

Protein extraction and LC-MS/MS analysis

In biological triplicates, 5×10⁶ amoebae were collected for each condition and centrifuged (500×g / 5 min / RT). The supernatant was discarded, and the pellet was resuspended in 20 mL of PAS buffer. The tube was centrifuged again (500×g / 5 min / RT). The supernatant was discarded, and the pellet was resuspended in 1.5 mL of PAS buffer and transferred to an Eppendorf microtube. The tubes were centrifuged again (500×g / 5 min / RT). The pellet was resuspended in 1.5 mL of extraction buffer (Tris-HCl 50 mM/ 8 M urea/ pH 8) and the

contents of the tubes were transferred to FastPrep-24™ 5G lysis tubes containing silica microbeads. Amoebae were mechanically lysed using a FastPrep-24™ 5G with the following settings: 3 steps of 30 sec at speed 6.0, with 5 min incubation on ice between each cycle. The lysates were then centrifuged (16,000×g / 10 min / 4°C) to remove cell debris. 1 mL of supernatant was transferred to a new tube and stored at -80°C before further analysis. An Amicon filter 3kDa (Sigma-Aldrich®) was used to reduce samples volume down to 100 µL, then disulfide bonds were reduced with 5 mM Tris(2-carboxyethyl) phosphine (TCEP) for 30 min and alkylated with 10 mM iodoacetamide for 30 min at room temperature (RT) in the dark. Proteins were digested using LysC (600 ng) for 3 h at 30°C and diluted with ammonium bicarbonate for down urea concentration inferior to 1 M. A second digestion step with Trypsin (800 ng) for 14 h at 37°C was performed. Digestion was stopped by adding 5% of formic acid (FA) and peptides were desalted and concentrated on a Sep-Pak light tC18 SPE cartridge (Waters) according to the manufacturer's instructions. Peptides were eluted using 50% acetonitrile (ACN), 0.1% FA. Purified peptides were lyophilized and kept at -80°C until further use.

The samples were resuspended in ACN 2%, FA 0.1% with a sonication step of 5 min. The samples were loaded and separated at 250 nL.min⁻¹ flow rates on a 30 cm HPLC column with C18 resin (1.9 µm particles, 100 Å pore size, Reprosil-Pur Basic C18-HD resin, Dr. Maisch GmbH) and equilibrated in 97% solvent A (H₂O, 0.1% FA) and 3% solvent B (ACN, 0.1% FA). Input sample peptides (proteome) were eluted with a buffer B linear gradient in 240 min. The MS/MS analysis was done on an Orbitrap Q Exactive plus Mass Spectrometer (ThermoFisher Scientific).

MaxQuant (v1.5.3.8) (Tyanova, Temu and Cox 2016) and the peptide search engine Andromeda (Cox *et al.* 2011) were used for protein identification with a custom-generated database constituted of the non-redundant protein sequences from the Uniprot *A. castellanii* strain Neff proteome. The Maxquant's label-free quantification (MaxLFQ) algorithm was used to calculate protein intensity profiles across samples (Cox *et al.* 2014).

An intensity value was quantified if at least 2 unique peptides were identified. Potential contaminants were deleted and only proteins with at least 2 quantified intensity values were kept. A false discovery rate (FDR) cutoff of 1% was applied at the peptide and protein levels.

The LFQ intensities values were used for Venn diagrams. Then, LFQ intensities values were log₂ transformed, normalized by average and slope followed by an imputation step to calculate missing values for fold-change (FC) and *p*-values calculation using the Aguilan *et al.* 2020 guide for proteomics (Aguilan, Kulej and Sidoli 2020). PCA analysis and heatmaps were performed with the relative intensities of proteins and using Metaboanalyst 5.0 (Pang *et al.* 2021). Functional Enrichment Analysis was performed using STRING v11.5 (<https://string-db.org>) (Szklarczyk *et al.* 2020) with proteins presenting a *p*-value < 0.05 thanks to their UniProt accession number and their FC against the site database called *Acanthamoeba castellanii* str. Neff with an FDR of 5%. Then lollipop plots were done with a cut-off of 10 proteins minimum for each GO term. Venn diagrams, volcano plots and lollipop plots were done using packages « ggVennDiagram » and « ggplot2 » with R v4.1.3 (03-10-2022).

Results and discussion

To understand how the *A. castellanii* proteome was altered by *L. pneumophila* infection, we used quantitative proteomic analysis following *A. castellanii* infection with *L. pneumophila* WT or $\Delta dotA$ at 24 and 48 h p.i. (Fig. 1A, Supplementary_Data_1_proteome_AC).

Overview of the temporal proteomic analysis of *A. castellanii* infected cells

First, a Venn diagram was made to highlight the distribution of proteins between every 5 experimental conditions (Fig. 1B), *i.e.* non-infected amoebae with 24 h of incubation at 30°C (NI 24 h), amoebae infected with *L. pneumophila* wild-type or $\Delta dotA$ at 24 h p.i. (Lp WT 24 h and Lp $\Delta dotA$ 24 h) or at 48 h p.i. (Lp WT 48 h and Lp $\Delta dotA$ 48 h). In total, 5921 proteins (around one-third of the total proteins based on the genome (Clarke *et al.* 2013) were identified among which 3815 (~65%) are common to the 5 conditions. We have observed that each condition presents specific proteins, 56 for NI 24 h, 41 for Lp $\Delta dotA$ 24 h against

125 at 48 h p.i. and 37 for Lp WT 24 h against 69 at 48 h p.i. Among these proteins specific to each condition, we have observed a noticeable proportion of uncharacterized proteins (from 25 to 37% approximately) compared to 19.5% of total proteins. Although we cannot explain why these proteins are uniquely linked to each condition, it would be interesting to perform further *in silico* analyses to determine the biological function of these uncharacterized proteins.

A first clustering analysis based on the relative intensities of the 5921 proteins was carried out between the different conditions (Fig. 1C). The heatmap shows the hierarchical proximity of the conditions at 24 h (NI 24 h, Lp WT 24 h, Lp $\Delta dotA$ 24 h). Moreover, NI and Lp $\Delta dotA$ 24 h presented similar protein profiles which seems to be justifiable by the fact that Lp $\Delta dotA$ has not a functional T4SS which makes it unable to multiply within *A. castellanii* (Bandyopadhyay *et al.* 2007). Lp WT 24 h has a protein profile different from NI and Lp $\Delta dotA$ 24 h possibly due to the effect of T4SS effectors.

However, it is also noted that NI, Lp $\Delta dotA$, and Lp WT show a certain variability in protein profile between the triplicates especially at 24 h post-infection. This variability within biological replicates at 24 h may be due to the absence of a centrifugation step for synchronization of infection. With the current protocol, the count of *L. pneumophila* CFU at 24 h and 48 h p.i. also led us to think that 48 h p.i. is the best time to observe the change in protein levels following the infection as more Lp WT seemed associated with amoebae (Fig. S1A). As expected, *Acanthamoeba* fed on the mutant $\Delta dotA$ which was not able to resist amoeba digestion (Fig. S1A). Although the counting of amoebae suggests a cell death in amoebae infected with Lp WT compared to those infected with Lp $\Delta dotA$ (Fig. S1B), the remaining amoebae infected by Lp WT were still viable (Fig. S1C).

Lp WT and Lp $\Delta dotA$ at 48 h p.i. showed less variability between the triplicates as well as diametrically different protein profiles. A second clustering approach using PCA was also reported (Fig. 1D) and confirmed the variability within the triplicates at 24 h. It also showed a diametrically opposite clustering according to principal component 1 for Lp $\Delta dotA$ and Lp WT

at 48 h and a good uniformity between biological replicates. Based on these 2 clustering analyses, we preferred to compare the different conditions separately regarding the time points (24 h then 48 h p.i.) in the rest of this study.

Regulation of amoebae protein upon infection

We then compared the conditions 2 by 2 through the FC associated with each protein by establishing the associated volcano plot (Fig. 2). Infection with *L. pneumophila* WT induced a decrease in levels for a majority of proteins. It was noted that infection with Lp WT led to 557 proteins with lower levels against 158 proteins with higher levels at 24 h p.i. compared to non-infected cells (Fig. 2A), whereas for Lp $\Delta dotA$ (Fig. 2B) these proteins numbers were 198 and 247 respectively. When amoebae are infected by Lp WT rather than Lp $\Delta dotA$, 465 proteins were detected with lower levels and 158 were detected with higher levels at 24 h p.i. (Fig. 2C). These protein numbers were 1264 and 639 at 48 h p.i. respectively (Fig. 2D). These results are consistent with the ability of *L. pneumophila* to reduce translation in eukaryotic cells including mammal and *A. castellanii* cells (Belyi *et al.* 2006, 2008; Shen *et al.* 2009; Moss *et al.* 2019).

Regarding the comparison between Lp $\Delta dotA$ and Lp WT, the levels of 10% (~600 proteins) of the total proteins were significantly modified at 24 h p.i. (Fig. 2C) while this proportion increases to 30% (~1900 proteins) at 48 h p.i. (Fig. 2D). This observation could be linked with the absence of synchronization of the infection added with T4SS effectors effects and the diminution Lp $\Delta dotA$ associated with amoebae that were more important at 48 h p.i. (Fig. S1A).

Gene ontology enrichment analysis of proteins regulated by the T4SS (Lp $\Delta dotA$ vs Lp WT 48 h p.i.)

To deepen the understanding of major functions modified during the infection of amoebae, GO term enrichment was assessed on the comparison between Lp $\Delta dotA$ and Lp WT 48 h p.i. (Fig. 3).

Biological processes

Regarding the enriched GO terms linked to the biological processes (Fig. 3A), we have noted a total of 22 enriched GO terms, among which 19 gathered proteins whose levels tends to be reduced and 3 gathered proteins whose levels tend to be increased.

There were 5 GO terms associated with lipid metabolism or homeostasis (GO:0055088; GO:0030258; GO:0008610; GO:0044255 and GO:0006629). We can also note that these 5 GO terms include proteins (10 to 111 proteins) that tend to have reduced levels and enrichment scores ranging from 1.8 to 4.5 (Fig. 3A). The modification of the lipid regulation of *A. castellanii* by *L. pneumophila* WT has been previously reported. Indeed, a subset of genes linked to lipid localization was upregulated following *A. castellanii* infection by *L. pneumophila* (Li *et al.* 2020). Our result suggests the capacity of *L. pneumophila* effectors to modulate the levels of proteins implicated in the lipid process of *A. castellanii*.

GO terms associated with signal transduction of small GTPase regulation (GO:0046578 and GO:0051056), gathered 11 and 18 proteins that tend to have reduced levels with an enrichment score of 3.1 and 4.1 (Fig. 3A). Many *Legionella* effectors modify eukaryotic small GTPases, which are involved in vesicular trafficking and membrane maturation in host cells (Goody and Itzen 2014; Hilbi *et al.* 2014; Spanò and Galán 2018). It has been shown that a subset of *A. castellanii* genes linked to small GTPases signaling was up-regulated by *L. pneumophila* at 24 h p.i. (Li *et al.* 2020). Here, we have found that proteins involved in small GTPases regulation were in lower levels in *A. castellanii* infected by *L. pneumophila* WT at 48 h p.i. This may be due to a more advanced stage of *L. pneumophila* presence in the LCV.

The GO terms associated with post-translational modifications (GO:0006468; GO:0000209), gathered 78 and 14 proteins that tend to have reduced levels for protein phosphorylation and increased levels for protein polyubiquitination with an enrichment score of 1.6 and 3.4 respectively (Fig. 3A). The ability of *L. pneumophila* to alter post-translational modifications has been previously described (Rolando and Buchrieser 2012). It seems that protein

phosphorylation tends to be diminished by *L. pneumophila* in *A. castellanii*. Regarding the increase in number of the proteins associated with polyubiquitination, it is known that *L. pneumophila* LCV presents polyubiquitinated proteins in HEK293T cells (Bruckert and Abu Kwaik 2015) that could explain in part the trend toward an increase in the polyubiquitination activity in *A. castellanii*.

Protein folding (GO:0006457), gathered 23 proteins with an enrichment score of 2.4, and proteolysis (GO:0006508) gathered 123 proteins with a score of 0.9 (Fig. 3A). They both included proteins that tend to have increased levels. Interestingly, little is known concerning the capacity of *L. pneumophila* to increase these host functions.

Molecular functions

Among enriched GO terms linked to molecular functions (Fig. 3B), we have reported a total of 29 enriched GO terms, 22 of those included proteins whose levels tend to be reduced and 7 included proteins whose levels tend to be increased.

Three GO terms associated with kinase activities (GO:0004674; GO:0004672; GO:0016301), gathering 73, 79, and 108 proteins that tend to have reduced levels with an enrichment score of 1.73, 1.67, and 1.51 respectively (Fig. 3B). It is known that phosphorylation is a predominant modification in *A. castellanii* (Clarke *et al.* 2013) and that diminution of phosphorylation is a rapid response when this amoeba is exposed to stress (Bernard *et al.* 2022). *L. pneumophila* effectors seem to be able to decrease host kinase activity in *A. castellanii*, which is consistent with transcriptomic data obtained previously with the same model (Moon *et al.* 2021).

GO term linked to the helicase activity (GO:0004386) gathered 32 proteins (Fig. 3B). These proteins tended to have reduced levels with a 2.3 enrichment score. Regarding the implication of helicase in transcription, our result is in agreement with what has been previously reported regarding the capacity of *L. pneumophila* to decrease the host's

transcription by targeting the RNA Polymerase II with SnpL or the chromatin with the methyltransferase RomA (Li *et al.* 2013; Rolando *et al.* 2013; Schuelein *et al.* 2018).

Focusing on GO terms with proteins that tend to have increased levels. One GO term is associated with antioxidant activity (GO:0016206) including 15 proteins with a score of 2.7 (Fig. 3B). It has already been shown the ability of *L. pneumophila* to reduce the amount of ROS in macrophages (Harada, Miyake and Imai 2007) and this result tends to suggest a reduction of ROS in *A. castellanii* infected with *L. pneumophila* WT.

Cellular components

It's well known that *L. pneumophila* can manipulate host cell organelles (Kellermann, Scharte and Hensel 2021). For enriched GO terms linked to cellular components (Fig. 3C), we have reported a total of 8 enriched GO terms, among which 7 included proteins whose levels tended to be reduced and 1 included protein whose levels tended to be increased.

Among them, two GO terms are related to the organelles (GO:0031984 and GO:0031090) including 14 and 176 proteins that tended to have reduced levels with 4 and 1.16 scores respectively. Among these proteins, we noticed proteins linked to the Golgi apparatus, ER, vesicle, or mitochondria. Alteration of normal vacuolar trafficking by *L. pneumophila* is well described in *A. castellanii* and *D. discoideum* with LegC2/YlfB and LegC7/YlfA (Campodonico, Chesnel and Roy 2005) as well as modulation of mitochondrial dynamics in macrophages thanks to MitF that promote a Warburg-like phenotype in macrophages (Escoll *et al.* 2017).

Two GO terms were related to the Golgi apparatus (GO:0098791 and GO:0005794) including 12 and 59 proteins that tend to have reduced levels with 3.6 and 2.4 scores respectively. It is known that *L. pneumophila* maintains and requires an intact host Golgi ultrastructure in infected macrophages (Fu *et al.* 2022). Nevertheless, our results suggest a decrease in the number of proteins linked to the Golgi apparatus in *A. castellanii* infected by *L. pneumophila*. 1 GO term is related to the Endoplasmic reticulum membrane

(GO:0005789) with 59 proteins that tend to have a negative FC and a score of 2.07. It is known that *L. pneumophila* uses SidC (Ragaz *et al.* 2008) and SidJ (Liu and Luo 2007) to recruit ER into the LCV of *D. discoideum*. Our result underlines the decrease in the protein levels linked to the ER membrane in *A. castellanii*.

Taken together, these results confirm the capacity of *L. pneumophila* to modify the levels of proteins linked to the organelles of *A. castellanii*. This is in adequation with transcriptomic results that have previously shown that *L. pneumophila* was able to modify the regulation of a subset of *A. castellanii* genes linked to ER to Golgi vesicle-mediated transport and mitochondrial respiratory chain complex III assembly (Li *et al.* 2020; Moon *et al.* 2021).

Conclusion

In conclusion, our study showed that *L. pneumophila* T4SS effectors induce a modification of the proteome of *A. castellanii* by inducing a drastic decrease in the protein level. Many of these proteins are linked to important physiological functions including lipid metabolism, post-modification regulations, kinase activities and helicase activities in addition to altering proteins related to organelles. This decrease might be due to the previously reported capacity of *Legionella* to inhibit the host translation, but also by an increase of proteins involved in proteolytic activities shown in this study. Interestingly, we also reported an increase in protein levels involved in antioxidant activities and protein folding. It is the first time that a global proteomic approach has been applied to *A. castellanii* infected by *L. pneumophila*. This study will lead to a more detailed exploration of the underlying mechanisms responsible for these changes allowing a better understanding of the interaction between *L. pneumophila* and *A. castellanii*.

Conflict of interest

None declared.

Bibliography

- Aguilan JT, Kulej K, Sidoli S. Guide for protein fold change and p -value calculation for non-experts in proteomics. *Mol Omics* 2020;**16**:573–82.
- Bandyopadhyay P, Liu S, Gabbai CB *et al.* Environmental mimics and the Lvh type IVA secretion system contribute to virulence-related phenotypes of *Legionella pneumophila*. *Infect Immun* 2007;**75**:723–35.
- Belyi Y, Niggeweg R, Opitz B *et al.* *Legionella pneumophila* glucosyltransferase inhibits host elongation factor 1A. *Proceedings of the National Academy of Sciences* 2006;**103**:16953–8.
- Belyi Y, Tabakova I, Stahl M *et al.* Lgt: a family of cytotoxic glucosyltransferases produced by *Legionella pneumophila*. *J Bacteriol* 2008;**190**:3026–35.
- Berjeaud J-M, Chevalier S, Schlüsselhuber M *et al.* *Legionella pneumophila*: The Paradox of a Highly Sensitive Opportunistic Waterborne Pathogen Able to Persist in the Environment. *Front Microbiol* 2016;**7**, DOI: 10.3389/fmicb.2016.00486.
- Bernard C, Locard-Paulet M, Noël C *et al.* A time-resolved multi-omics atlas of *Acanthamoeba castellanii* encystment. *Nat Commun* 2022;**13**:4104.
- Bruckert WM, Abu Kwaik Y. Complete and ubiquitinated proteome of the *Legionella*-containing vacuole within human macrophages. *J Proteome Res* 2015;**14**:236–48.
- Campodonico EM, Chesnel L, Roy CR. A yeast genetic system for the identification and characterization of substrate proteins transferred into host cells by the *Legionella pneumophila* Dot/Icm system. *Molecular Microbiology* 2005;**56**:918–33.
- Cazalet C, Rusniok C, Brüggemann H *et al.* Evidence in the *Legionella pneumophila* genome for exploitation of host cell functions and high genome plasticity. *Nat Genet* 2004;**36**:1165–73.
- Chauhan D, Shames SR. Pathogenicity and Virulence of *Legionella*: Intracellular replication and host response. *Virulence* 2021;**12**:1122–44.
- Clarke M, Lohan AJ, Liu B *et al.* Genome of *Acanthamoeba castellanii* highlights extensive lateral gene transfer and early evolution of tyrosine kinase signaling. *Genome Biology* 2013;**14**:R11.
- Cosson P, Soldati T. Eat, kill or die: when amoeba meets bacteria. *Curr Opin Microbiol* 2008;**11**:271–6.
- Cox J, Hein MY, Lubner CA *et al.* Accurate Proteome-wide Label-free Quantification by Delayed Normalization and Maximal Peptide Ratio Extraction, Termed MaxLFQ. *Mol Cell Proteomics* 2014;**13**:2513–26.
- Cox J, Neuhauser N, Michalski A *et al.* Andromeda: A Peptide Search Engine Integrated into the MaxQuant Environment. *J Proteome Res* 2011;**10**:1794–805.

- Escoll P, Song O-R, Viana F *et al.* Legionella pneumophila Modulates Mitochondrial Dynamics to Trigger Metabolic Repurposing of Infected Macrophages. *Cell Host Microbe* 2017;**22**:302-316.e7.
- Fouque E, Trouilhé M-C, Thomas V *et al.* Cellular, Biochemical, and Molecular Changes during Encystment of Free-Living Amoebae. *Eukaryot Cell* 2012;**11**:382–7.
- Fu Y, Macwan V, Heineman RE-S *et al.* Legionella pneumophila Infection of Human Macrophages Retains Golgi Structure but Reduces O-Glycans. *Pathogens* 2022;**11**:908.
- Gomez-Valero L, Rusniok C, Carson D *et al.* More than 18,000 effectors in the Legionella genus genome provide multiple, independent combinations for replication in human cells. *Proc Natl Acad Sci U S A* 2019;**116**:2265–73.
- Gomez-Valero L, Rusniok C, Rolando M *et al.* Comparative analyses of Legionella species identifies genetic features of strains causing Legionnaires' disease. *Genome Biol* 2014;**15**:505.
- Goody RS, Itzen A. Modulation of Small GTPases by Legionella. In: Hilbi H (ed.). *Molecular Mechanisms in Legionella Pathogenesis*. Berlin, Heidelberg: Springer, 2014, 117–33.
- Harada T, Miyake M, Imai Y. Evasion of *Legionella pneumophila* from the Bactericidal System by Reactive Oxygen Species (ROS) in Macrophages. *Microbiology and Immunology* 2007;**51**:1161–70.
- Hilbi H, Rothmeier E, Hoffmann C *et al.* Beyond Rab GTPases Legionella activates the small GTPase Ran to promote microtubule polymerization, pathogen vacuole motility, and infection. *Small GTPases* 2014;**5**:1–6.
- Isaac DT, Isberg R. Master manipulators: an update on Legionella pneumophila Icm/Dot translocated substrates and their host targets. *Future Microbiol* 2014;**9**:343–59.
- de Jesús-Díaz DA, Murphy C, Sol A *et al.* Host Cell S Phase Restricts Legionella pneumophila Intracellular Replication by Destabilizing the Membrane-Bound Replication Compartment. *mBio* 2017;**8**:e02345-16.
- Kellermann M, Scharte F, Hensel M. Manipulation of Host Cell Organelles by Intracellular Pathogens. *Int J Mol Sci* 2021;**22**:6484.
- Kunze M, Steiner T, Chen F *et al.* Metabolic adaption of Legionella pneumophila during intracellular growth in Acanthamoeba castellanii. *International Journal of Medical Microbiology* 2021;**311**:151504.
- Li P, Vassiliadis D, Ong SY *et al.* Legionella pneumophila Infection Rewires the Acanthamoeba castellanii Transcriptome, Highlighting a Class of Sirtuin Genes. *Front Cell Infect Microbiol* 2020;**10**:428.
- Li T, Lu Q, Wang G *et al.* SET-domain bacterial effectors target heterochromatin protein 1 to activate host rDNA transcription. *EMBO reports* 2013;**14**:733–40.
- Liu Y, Luo Z-Q. The Legionella pneumophila effector SidJ is required for efficient recruitment of endoplasmic reticulum proteins to the bacterial phagosome. *Infect Immun* 2007;**75**:592–603.

- Maita C, Matsushita M, Miyoshi M *et al.* Amoebal endosymbiont Neochlamydia protects host amoebae against Legionella pneumophila infection by preventing Legionella entry. *Microbes and Infection* 2018;**20**:236–44.
- Mengue L, Régnacq M, Aucher W *et al.* Legionella pneumophila prevents proliferation of its natural host Acanthamoeba castellanii. *Sci Rep* 2016;**6**:36448.
- Mengue L, Richard F-J, Caubet Y *et al.* Legionella pneumophila decreases velocity of Acanthamoeba castellanii. *Exp Parasitol* 2017;**183**:124–7.
- Moon E-K, Park S-M, Chu K-B *et al.* Differentially Expressed Gene Profile of Acanthamoeba castellanii Induced by an Endosymbiont Legionella pneumophila. *Korean J Parasitol* 2021;**59**:67–75.
- Moss SM, Taylor IR, Ruggero D *et al.* A Legionella pneumophila Kinase Phosphorylates the Hsp70 Chaperone Family to Inhibit Eukaryotic Protein Synthesis. *Cell Host & Microbe* 2019;**25**:454-462.e6.
- Pang Z, Chong J, Zhou G *et al.* MetaboAnalyst 5.0: narrowing the gap between raw spectra and functional insights. *Nucleic Acids Research* 2021;**49**:W388–96.
- Ragaz C, Pietsch H, Urwyler S *et al.* The Legionella pneumophila phosphatidylinositol-4 phosphate-binding type IV substrate SidC recruits endoplasmic reticulum vesicles to a replication-permissive vacuole. *Cell Microbiol* 2008;**10**:2416–33.
- Rolando M, Buchrieser C. Post-translational modifications of host proteins by Legionella pneumophila: a sophisticated survival strategy. *Future Microbiol* 2012;**7**:369–81.
- Rolando M, Sanulli S, Rusniok C *et al.* Legionella pneumophila Effector RomA Uniquely Modifies Host Chromatin to Repress Gene Expression and Promote Intracellular Bacterial Replication. *Cell Host & Microbe* 2013;**13**:395–405.
- Samba-Louaka A. Amoebae as Targets for Toxins or Effectors Secreted by Mammalian Pathogens. *Toxins* 2021;**13**:526.
- Samba-Louaka A, Delafont V, Rodier M-H *et al.* Free-living amoebae and squatters in the wild: ecological and molecular features. *FEMS Microbiol Rev* 2019;**43**:415–34.
- Schuelein R, Spencer H, Dagley LF *et al.* Targeting of RNA Polymerase II by a nuclear Legionella pneumophila Dot/lcm effector SnpL. *Cellular Microbiology* 2018;**20**:e12852.
- Schunder E, Gillmaier N, Kutzner E *et al.* Amino Acid Uptake and Metabolism of Legionella pneumophila Hosted by Acanthamoeba castellanii. *J Biol Chem* 2014;**289**:21040–54.
- Shen X, Banga S, Liu Y *et al.* Targeting eEF1A by a Legionella pneumophila effector leads to inhibition of protein synthesis and induction of host stress response. *Cellular Microbiology* 2009;**11**:911–26.
- Simon S, Schell U, Heuer N *et al.* Inter-kingdom Signaling by the Legionella Quorum Sensing Molecule LAI-1 Modulates Cell Migration through an IQGAP1-Cdc42-ARHGEF9-Dependent Pathway. *PLOS Pathogens* 2015;**11**:e1005307.
- Spanò S, Galán JE. Taking control: Hijacking of Rab GTPases by intracellular bacterial pathogens. *Small GTPases* 2018;**9**:182–91.

Swart AL, Harrison CF, Eichinger L *et al.* Acanthamoeba and Dictyostelium as Cellular Models for Legionella Infection. *Front Cell Infect Microbiol* 2018;**8**:61.

Szklarczyk D, Gable AL, Nastou KC *et al.* The STRING database in 2021: customizable protein–protein networks, and functional characterization of user-uploaded gene/measurement sets. *Nucleic Acids Res* 2020;**49**:D605–12.

Tyanova S, Temu T, Cox J. The MaxQuant computational platform for mass spectrometry-based shotgun proteomics. *Nat Protoc* 2016;**11**:2301–19.

Yang J-L, Li D, Zhan X-Y. Concept about the Virulence Factor of Legionella. *Microorganisms* 2022;**11**:74.

ORIGINAL UNEDITED MANUSCRIPT

Fig. 1

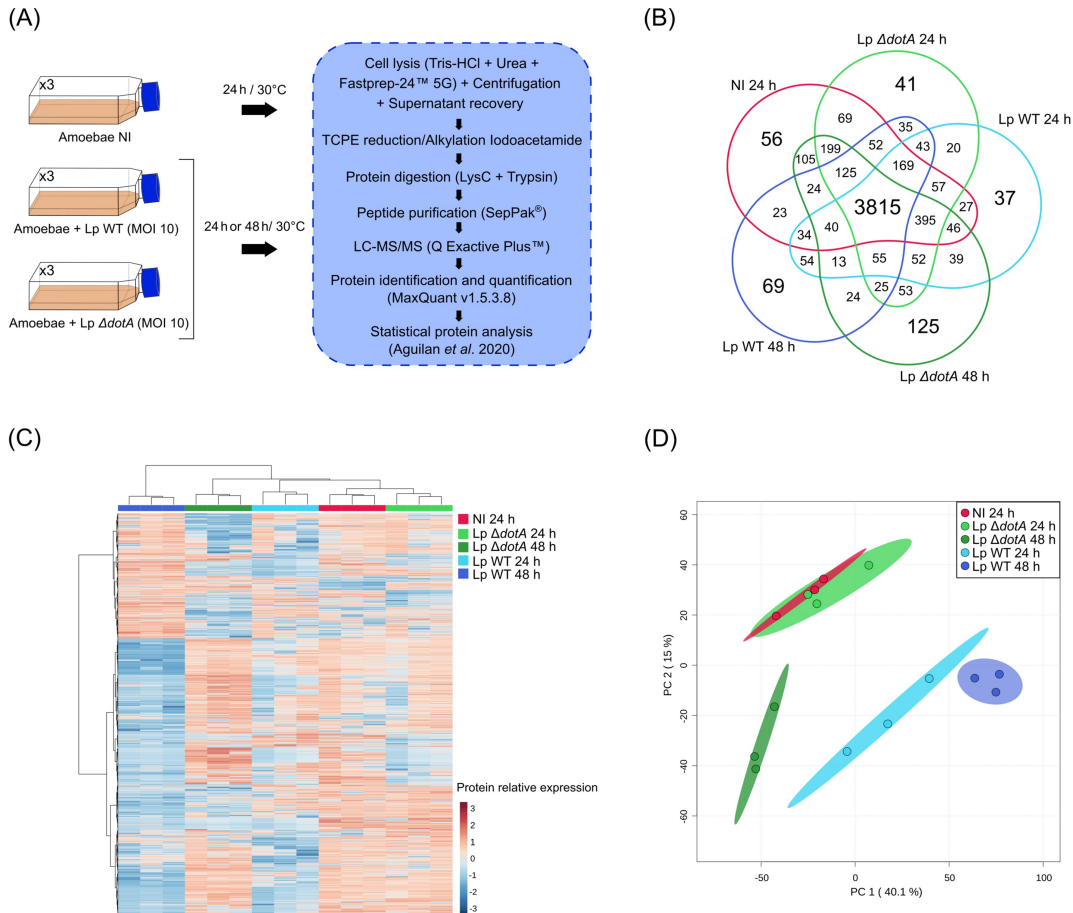


Fig. 1 Obtention and global comparison of an *A. castellanii* proteome following infection by *L. pneumophila*. (A) Schematic diagram of the experimental procedure used for the proteomic analysis of non-infected (NI) *A. castellanii* or infected with *L. pneumophila* wild-type (Lp WT) or *dotA* deficient (Lp $\Delta dotA$) at 24 or 48 h post-infection. (B) Venn diagram of the distribution of proteins per condition. (C) Heatmap diagram showing relative protein abundance changes between each condition using normalized protein intensity. Intensity levels higher and lower than the mean (white) are indicated in red and blue shades, respectively. (D) PCA score plot generated using MetaboAnalyst 5.0 with the same method used for (C).

Fig. 2

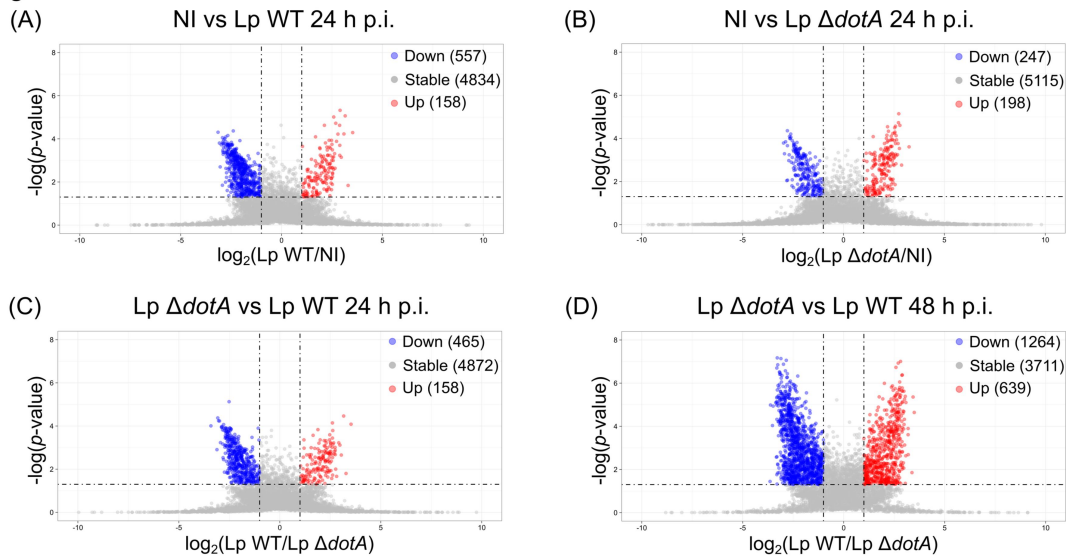


Fig. 2 Abundance of *A. castellanii* proteins using Volcano plots showing fold change (in \log_2).

The protein abundance of Non-infected (NI) cells is compared to those of infected cells with *L. pneumophila* wild-type (Lp WT) (A) or *L. pneumophila dotA* deficient (Lp $\Delta dotA$) (B). The abundance of proteins in infected cells with Lp $\Delta dotA$ is compared to those of infected cells with Lp WT at 24 h (C) and 48 h post-infection (D). Dashed lines correspond to the fixed limits of p-value and fold-change, 0.05 and 2 respectively. More abundant proteins (Up) are represented by a red dot and those that are less abundant (Down) by a blue dot and stable proteins (Stable) are represented by a grey dot. The total of proteins for each category is indicated between parentheses.

Fig. 3

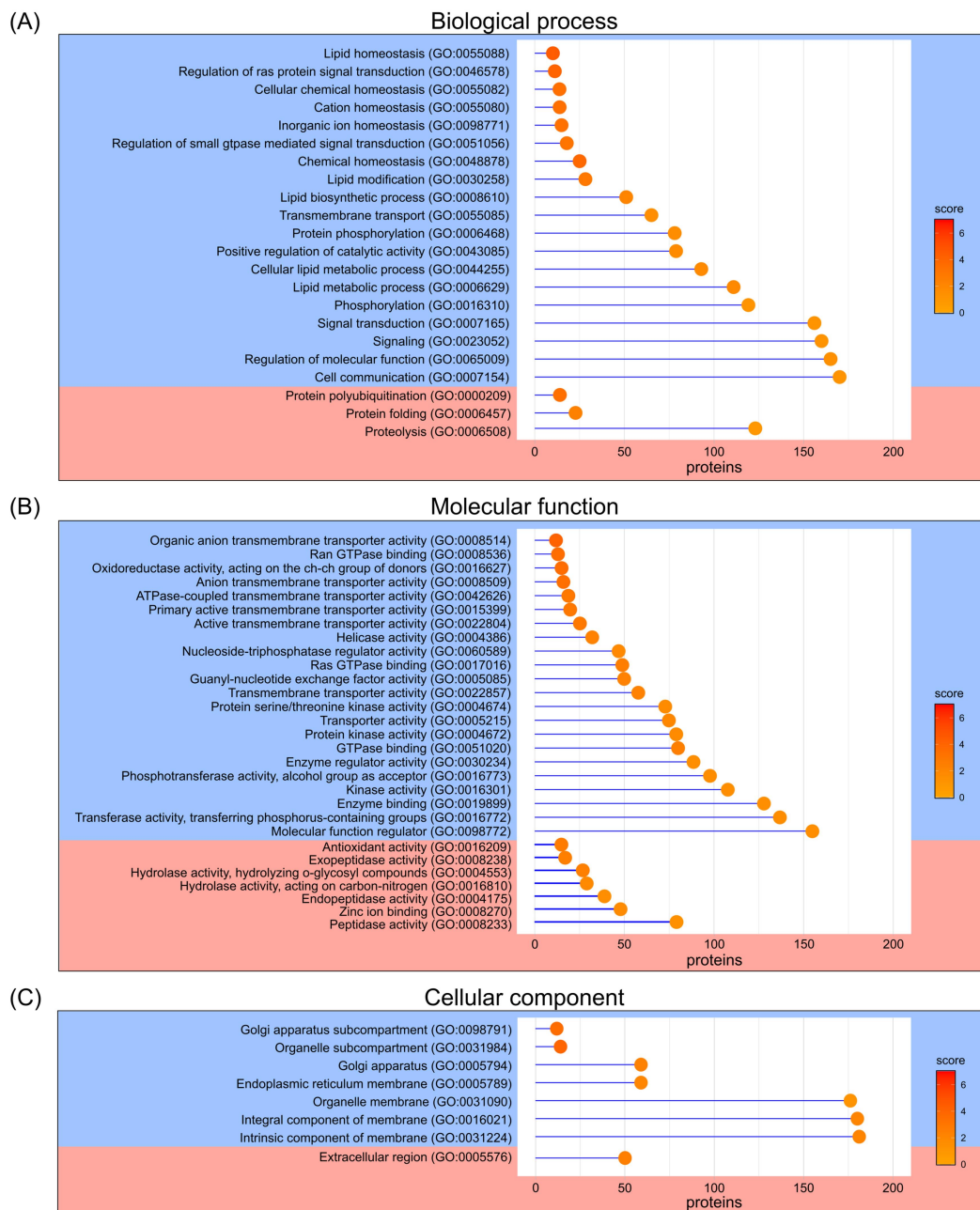
Lp $\Delta dotA$ vs Lp WT 48 h

Fig. 3 GO terms enriched in infected cells with *L. pneumophila* $\Delta dotA$ versus *L. pneumophila* wild-type 48 h post-infection. Lollipop plot of Gene Ontology (GO) terms enrichment for biological process (A) molecular function (B) and cellular component (C). The number of

ORIGINAL

proteins in each GO term is indicated by the stick's length, and the ball represents the enrichment score obtained by a shade of red. The enrichment score corresponds to the absolute value of the ratio between the difference between the average fold-changes of the GO term and the average fold-changes in the database, and the maximum deviation from the mean in the database, multiplied by 10. The pale blue part included GO terms that present proteins that tend to have negative fold-change and the pale red part those that present proteins that tend to have positive fold-change.

ORIGINAL UNEDITED MANUSCRIPT